

Learn by Reasoning: Analogical Weight Generation for Few-Shot Class-Incremental Learning

Jizhou Han, Chenhao Ding, Yuhang He, Songlin Dong, Qiang Wang, Xinyuan Gao, Yihong Gong[†], *Fellow, IEEE*

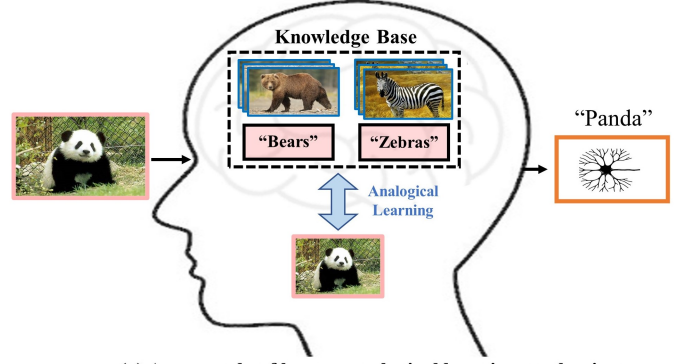
Abstract—Few-shot class-incremental Learning (FSCIL) enables models to learn new classes from limited data while retaining performance on previously learned classes. Traditional FSCIL methods often require fine-tuning parameters with limited new class data and suffer from a separation between learning new classes and utilizing old knowledge. Inspired by the analogical learning mechanisms of the human brain, we propose a novel analogical generative method. Our approach includes the Brain-Inspired Analogical Generator (BiAG), which derives new class weights from existing classes without parameter fine-tuning during incremental stages. BiAG consists of three components: Weight Self-Attention Module (WSA), Weight & Prototype Analogical Attention Module (WPAA), and Semantic Conversion Module (SCM). SCM uses Neural Collapse theory for semantic conversion, WSA supplements new class weights, and WPAA computes analogies to generate new class weights. Experiments on miniImageNet, CUB-200, and CIFAR-100 datasets demonstrate that our method achieves higher final and average accuracy compared to SOTA methods.

Index Terms—Few-shot class-incremental learning, Analogical learning, Brain-inspired model, Classifier weight generation, Attention mechanism

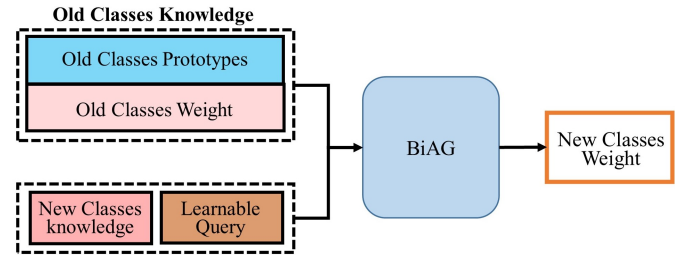
I. INTRODUCTION

Conventional deep learning models have achieved remarkable success in various computer vision and pattern recognition tasks. However, these models are typically developed under a closed-world assumption, where all categories are predefined, and ample labeled data is available for each class. In practice, this assumption rarely holds. New classes may appear continuously over time, while labeled data is often expensive or difficult to obtain. To address this limitation, Class-Incremental Learning (CIL) has been proposed to enable models to learn new categories sequentially while retaining prior knowledge. Although effective in fully supervised settings, most existing CIL methods assume sufficient data for each new class and often require storing exemplars from past sessions. These assumptions greatly limit their applicability in dynamic and data-constrained environments.

In many real-world scenarios, such as identifying rare species, adapting to evolving user behavior, or updating clinical diagnosis systems, new categories often emerge under tight time constraints and with very limited data. In such settings, retraining models from scratch or storing all historical data is often infeasible. Moreover, traditional CIL methods tend to overfit to the few new samples or suffer from forgetting previously learned knowledge. To address these challenges, Few-Shot Class-Incremental Learning (FSCIL) has been proposed [1]. FSCIL requires models to learn new classes from only a handful of labeled examples while maintaining performance on old classes. Typically, the model is trained



(a) An example of human analogical learning mechanism



(b) Illustration of the Brain-Inspired Analogical Generator (BiAG).

Fig. 1. An example of human analogical learning mechanism and the proposed Brain-Inspired Analogical Generator (BiAG). (a) Humans can efficiently form concepts of new categories through analogical reasoning. For example, when encountering a new animal like a panda, one may relate its visual characteristics to previously known categories—such as the body shape of a bear and the black-and-white color pattern of a zebra. This analogy enables the construction of a concept of “panda” even from limited samples. (b) Inspired by this cognitive mechanism, our BiAG module analogically generates classification weights for new classes by leveraging prototypes and weights from old classes along with a learnable query derived from new class knowledge. This allows efficient integration of new categories in few-shot incremental learning.

in a base session with sufficient data, followed by multiple incremental sessions with only a few examples per new class. Data from previous sessions becomes unavailable, and the model must perform classification over all seen classes. This setting emphasizes the need for methods that can effectively balance stability and plasticity under strict data and time constraints.

FSCIL faces two major challenges: overfitting caused by the limited training samples of new classes and catastrophic forgetting of old classes [1]. Existing methods can be broadly categorized into unified learning approaches and sequential learning approaches. Unified learning methods aim to jointly optimize for both new and old classes by leveraging retained

old knowledge. For example, meta-learning-based methods [2], [3] enhance adaptability by utilizing knowledge from related tasks, while replay-based methods [4] mitigate forgetting by replaying previously learned information. Dynamic network structures [5] employ adaptive graph models to better integrate new and old knowledge. On the other hand, sequential learning approaches treat the learning of new classes and the retention of old knowledge as separate tasks. Some of these methods focus on efficient representation learning to address the challenge of limited data [6], [7], [8]. Despite their merits, both approaches suffer from common limitations. First, they often rely on fine-tuning during incremental stages, which increases the risk of overfitting to the limited samples of new classes. Second, these methods treat the learning of new classes and the retention of old knowledge as separate tasks, resulting in a disconnect between the utilization of new and old knowledge. This separation makes it challenging to achieve a balanced integration of old knowledge retention and new information acquisition.

In contrast, humans excel in learning new concepts by leveraging prior knowledge through *analogical reasoning*. Rather than isolating new and old information, humans draw connections between existing knowledge and new information to efficiently construct new concepts [9], [10]. Cognitive science research highlights that analogical reasoning plays a vital role in human learning. The hippocampus converts short-term memories into long-term memories stored in the cerebral cortex, forming a comprehensive knowledge base [11]. When humans encounter new concepts, this knowledge base is accessed to retrieve relevant prior experiences. Regions such as the prefrontal cortex and anterior temporal lobes facilitate the process by drawing analogies between new information and existing knowledge [12]. This analogical reasoning process is further supported by the formation of new synapses, which create neural pathways enabling the brain to integrate and generate new concepts [13]. For example, as shown in Fig. 1(a), when learning a new concept like a "panda," humans draw upon prior knowledge of related concepts such as "bear" and "zebra," leveraging similarities to efficiently construct the concept of "panda" even with minimal samples.

Inspired by the analogical learning mechanism of the human brain, we propose a novel analogical generation method that derives new class weights from existing ones. Our method sufficiently utilizes prior knowledge during incremental sessions while eliminating the need for parameter training. The framework includes a feature extractor and a Brain-Inspired Analogical Generator (BiAG). The BiAG takes the prototypes (the centric or mean feature of an identical class) of new and old classes, as well as the classification weights of old classes, as inputs to the module, and outputs the generated classification weights of the new classes. The BiAG comprises three core components: the Semantic Conversion Module (SCM), the Weight Self-Attention Module (WSA), and the Weight & Prototype Analogical Attention Module (WPAA). The SCM facilitates smooth transitions between prototypes and classification weights based on Neural Collapse theory. The WSA enhances old knowledge utilization by supplementing new class weights, while the WPAA draws

analogies between old and new classes, reorganizing old weights to generate accurate new class weights. Building upon this foundation, our framework is structured into two distinct phases: the *base session training* and *incremental session inference* phases. During the base session, the feature extractor is trained on the base classes to obtain initial classification weights and prototypes, thereby constructing the knowledge base for analogical learning. Subsequently, the BiAG is trained to cultivate the ability to generate weights for novel classes through simulated incremental learning, wherein we randomly divide the base classes into old and new classes and train the model to generate weights for new classes. In the incremental inference phase, as illustrated in Fig. 1(b), the BiAG generates new class weights by leveraging the prototypes of the new classes alongside the prototypes and weights of the old classes.

Compared to previous methods, the proposed analogical generation approach offers a more efficient and balanced integration of new class learning and old knowledge retention, eliminating the need for parameter fine-tuning during incremental learning stages. The main contributions are summarized as follows:

- We propose a novel analogical learning framework for FSCIL inspired by the human brain's analogical reasoning mechanism. By mimicking the cognitive process of drawing analogies between prior knowledge and new information, our framework offers an efficient and adaptive approach to incremental learning.
- We develop the BiAG, which uses old class knowledge, new class knowledge, and a learnable query to generate new class weights without parameter fine-tuning during incremental sessions.
- Experiments on three benchmark datasets demonstrate that our method achieves higher final and average accuracy compared to the current SOTA methods.

II. RELATED WORK

A. Class-Incremental Learning (CIL)

Class-incremental learning (CIL) enables models to continually recognize new classes while preserving knowledge of previously learned ones. The main challenge lies in *catastrophic forgetting*, where learning new tasks interferes with old knowledge. To address this, a variety of strategies have been developed. Regularization-based methods [14], [15], [16] penalize changes to important parameters to preserve past knowledge. For example, EWC [16] leverages Fisher Information to identify critical weights. More recent efforts introduce forgetting-aware directions and equilibrium constraints to improve stability [17]. Replay-based methods [18], [19], [20], [21] retain exemplars or use generative models [22] to rehearse previous classes. To overcome memory and privacy concerns, recent approaches replace exemplars with mixed features and auxiliary classes [23] or use semantic mapping and background calibration to improve alignment [24]. Statistical sampling has also been proposed to simulate past data distributions without real samples [25]. Parameter isolation strategies [26], [27], [28], [29] assign different parameter subsets to different tasks, avoiding interference. Pack-Net [27], for instance, uses weight pruning and reallocation

to accommodate new tasks efficiently. Dynamic architecture methods [30], [31], [32], [33] incrementally grow the network to handle new tasks, though often at the cost of increased complexity. Recent improvements include lightweight incremental frameworks [34] and memory-boosted transformers [35]. In addition, several works enhance representation quality to improve learning efficiency. For example, feature expansion and robust training techniques have proven effective in exemplar-free settings [36], while others leverage external semantic knowledge to guide feature learning and improve generalization [37].

Although these methods perform well on standard benchmarks, they typically rely on ample labeled data and access to prior tasks—conditions not met in few-shot class-incremental learning (FSCIL). In such scenarios, regularization may underfit, replay can overfit, and dynamic structures may be excessive. These limitations highlight the need for more efficient and generalizable CIL approaches under limited supervision.

B. Few-Shot Class-Incremental Learning (FSCIL)

Few-shot class-incremental learning (FSCIL) aims to learn new classes from few samples over time without forgetting old ones. Early works such as TOPIC [1] and CEC [5] adopt feature structure preservation or graph-based adaptation. Meta-learning-based methods like MetaFSCIL [3] and Self-promoted [38] improve adaptability via task sampling and prototype refinement. SPPR [39] and IDLVQ [40] enhance prototype-based learning through episodic sampling and vector quantization. To address representation degradation, FACT [41] pre-allocates virtual prototypes, while Data-free Replay [7] replays knowledge to balance class learning. LIMIT [42] and CLOM [43] employ transformers and margin constraints to align semantics and reduce overfitting. GKEAL [44] uses Gaussian kernels for analytic learning, and BiDist [45] distills knowledge from dual teachers. SVAC [8] enhances generalization via virtual classes. Dynamic model-based approaches include SubNet [46], WaRP [47], and KRRM [48], each tailoring model structures for incremental adaptation. NC-FSCIL [49] pre-assigns classifiers based on Neural Collapse, while ALICE [50] and OrCo [51] improve intra-class compactness and generalization via angular loss or orthogonality. YourSelf [52] uses pseudo-label self-training without fine-tuning. While ALFSCIL [53] explores analogical learning, it only leverages prototypes and still relies on fine-tuning. In contrast, our method, BiAG, fully utilizes both prototypes and old class weights to analogically generate new classifiers in a scalable and tuning-free manner.

C. Analogical Learning Mechanism

Analogical learning is a fundamental aspect of human cognition, allowing individuals to transfer knowledge from familiar domains (source) to novel situations (target) by recognizing relational similarities. This mechanism supports efficient and flexible learning and has been identified by cognitive science as a key driver of human intelligence [9], [10], [54]. According to Gentner’s Structure-Mapping Theory [55], analogical reasoning involves retrieving relevant experiences,

aligning relational structures (mapping), projecting inferences, evaluating consistency, and re-representing knowledge when necessary.

Neurologically, analogical reasoning is supported by a distributed network involving the hippocampus, prefrontal cortex (PFC), and anterior temporal lobes. The hippocampus transforms short-term experiences into long-term memories stored in the cortex [11], serving as a knowledge base for analogical retrieval. The left frontopolar cortex and inferior PFC aid in semantic processing and relational integration, while the right dorsolateral PFC supports inference and decision-making [12], [56]. The anterior temporal lobes further assist in linking new stimuli with prior knowledge. At the cellular level, analogical learning involves the formation of new synaptic pathways, enabling the integration and abstraction of novel concepts [13]. Inspired by these principles, we propose a brain-inspired analogical generator that emulates this mechanism for few-shot class-incremental learning.

III. METHOD

A. Problem Setting

Few-shot class-incremental Learning (FSCIL) aims to continuously learn new classes from a few examples while retaining previously acquired knowledge across multiple sessions. Assume we have a stream of labeled training sets $\{\mathcal{D}^0, \dots, \mathcal{D}^t, \dots, \mathcal{D}^T\}$ and test sets $\{\mathcal{Z}^0, \dots, \mathcal{Z}^t, \dots, \mathcal{Z}^T\}$, where T is the total number of incremental sessions. The training set $\mathcal{D}^t = \{(x_i^t, y_i^t) \mid i = 1, \dots, |\mathcal{D}^t|\}$ contains samples x_i^t and their corresponding labels $y_i^t \in \mathcal{C}^t$, where \mathcal{C}^t represents the classes in the t -th session. The same applies to the test set $\mathcal{Z}^t = \{(z_i^t, y_i^t) \mid i = 1, \dots, |\mathcal{Z}^t|\}$. For all i, j and $i \neq j$, $\mathcal{C}^i \cap \mathcal{C}^j = \emptyset$. The first training session is called the base session, where the training set \mathcal{D}^0 contains a sufficient number of examples for each class $c \in \mathcal{C}^0$. For any other session $t > 0$, \mathcal{D}^t is an N -way K -shot training set, containing N classes and K training examples for each class $c \in \mathcal{C}^t$. At the end of each training session t , the model is evaluated using the combined test set $\mathcal{Z}^{0:t} = \mathcal{Z}^0 \cup \dots \cup \mathcal{Z}^t$.

B. Framework Overview

As shown in Fig.2, our method consists of a feature extractor $f(\cdot)$, a Brain-Inspired Analogical Generator (BiAG) $\varphi_{\text{BiAG}}(\cdot)$, and linear classification weights W . In the training phase, the **Knowledge Base Construction** and **Analogical Generator Training** stages are involved. Initially, in the **Knowledge Base Construction** stage, the feature extractor $f(\cdot)$ is first trained on the \mathcal{D}^0 to obtain classification weights and prototypes for the base classes \mathcal{C}^0 . In the subsequent **Analogical Generator Training** stage, BiAG is trained to have the capability of generating new class weights through analogy by employing pseudo-incremental training and a loss function \mathcal{L}_G to ensure that the generated weights closely match the true weights. In the incremental phase, corresponding to the **Weight Generation for Newly Emerged Classes** stage, when new classes emerge, we use the trained feature extractor $f(\cdot)$ to extract prototypes of the new classes. BiAG $\varphi_{\text{BiAG}}(\cdot)$ then generates weights for the new classes by leveraging these new

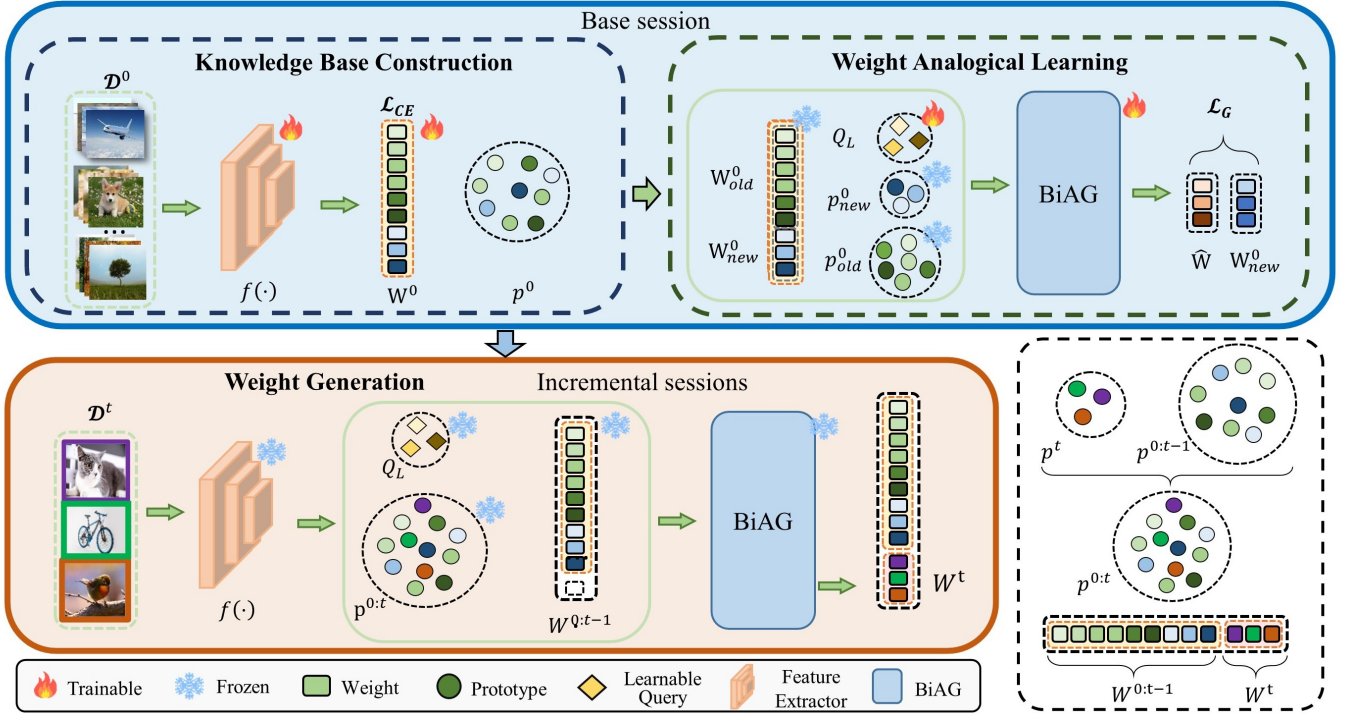


Fig. 2. **An overview of the proposed Analogical Generative Method.** *Knowledge Base Construction:* The network is trained to obtain classification weights and prototypes for the base classes. *Analogical Generator Training:* The BiAG uses pseudo-incremental training and \mathcal{L}_G to ensure that generated weights match true weights. *Weight Generation:* In the t -th session, BiAG generates weights for the new classes using new class prototypes, old class prototypes, and old class weights.

prototypes along with those from old classes and the weights of the old classes. During this phase, the parameters of both BiAG and the feature extractor are frozen.

1) *Knowledge Base Construction:* This stage simulates the hippocampus's function of converting short-term memories into a long-term repository of relational knowledge. BiAG first constructs a structured knowledge base by training a feature extractor on base classes. This process generates prototypes that encapsulate the central features of each class, providing a foundation for relational mapping. These prototypes act as a semantic bridge, facilitating the integration of new class information without disrupting existing representations.

In the base session, we use \mathcal{D}^0 that contains sufficient data to train the feature extractor $f(\cdot)$ for knowledge base construction. We optimize the model through sample loss during training:

$$\mathcal{L}_{cls} = - \sum_{i=1}^{N_{D^0}} y_i^0 \log \left(\frac{\exp(h_W(f(x_i^0)))}{\sum_{j=1}^{|\mathcal{C}^0|} \exp(h_W(f(x_j^0)))} \right) \quad (1)$$

where, $h_W(\cdot)$ is the linear classification layer and $f(\cdot)$ denotes the feature extractor. N_{D^0} is the number of the samples of \mathcal{D}^0 . N_{C^j} denotes the number of the samples of \mathcal{C}^j .

After the training is completed, we freeze $f(\cdot)$ to alleviate catastrophic forgetting and save the classification weights W^0 of base classes for subsequent processes. The feature extractor remains frozen in all subsequent stages.

2) *Analogical Generator Training:* In this stage, BiAG is trained to have the capability of generating new class weights

through analogy. To achieve this goal, we take the following steps:

First, we obtain prototypes p^0 for all base classes \mathcal{C}^0 using the feature extractor $f(\cdot)$. The prototypes p^0 are the average embeddings for each class, calculated as follows:

$$p_{c_i} = \frac{1}{N_{c_i}} \sum_{j=1}^{N_{c_i}} f(x_{j,c_i}) \quad (2)$$

where x_{j,c_i} is the j -th sample of class c_i , and N_{c_i} is the number of samples of class c_i .

Next, in each round of training, we randomly divide the base classes \mathcal{C}^0 into pseudo-old classes \mathcal{C}_{old}^0 and pseudo-new classes \mathcal{C}_{new}^0 , ensuring $\mathcal{C}_{old}^0 \cap \mathcal{C}_{new}^0 = \emptyset$. Based on this division, we also split p^0 into p_{old}^0 and p_{new}^0 , and W^0 into W_{old}^0 and W_{new}^0 . We define the generated class weights as $G = \{g_{c_i}\}_{i=1}^{|\mathcal{C}_{new}^0|}$ ($c_i \in \mathcal{C}_{new}^0$). Then we employ the BiAG to generate the G with p_{old}^0 , p_{new}^0 , and W_{old}^0 :

$$G = \varphi_{\text{BiAG}}(p_{old}^0, p_{new}^0, W_{old}^0) p_{c_i} = \frac{1}{N_{c_i}} \sum_{j=1}^{N_{c_i}} f(x_{j,c_i}) \quad (3)$$

where $\varphi_{\text{BiAG}}(\cdot)$ denotes BiAG, and details about BiAG will be elaborated in 3.3. To ensure the stability and accuracy of G , we use cosine similarity between G and W_{new}^0 to constrain G :

$$\mathcal{L}_G = 1 - \frac{G \cdot W_{new}^0{}^T}{\|G\| \cdot \|W_{new}^0\|} \quad (4)$$

where W_{new}^0 is the classification weight in W^0 corresponding to class \mathcal{C}_{new}^0 .

Algorithm 1 Our Method Framework

```

1: Step 1: Knowledge Base Construction (Base Session)
2: for each epoch in base session training do
3:   Train feature extractor  $f(\cdot)$  and classifier on  $\mathcal{D}^0$ 
4: end for
5: Compute prototypes  $\mathbf{p}^0$  using  $f(\cdot)$  ▷ Eq.(2)
6: Save classification weights  $W^0$  and freeze  $f(\cdot)$ 

7: Step 2: Analogical Generator Training
8: for each epoch in BiAG training do
9:   Randomly split  $\mathcal{C}^0$  into  $\mathcal{C}_{old}^0$  and  $\mathcal{C}_{new}^0$ 
10:  Get prototypes  $\mathbf{p}_{old}^0, \mathbf{p}_{new}^0$ , and weights  $W_{old}^0, W_{new}^0$ 
11:  Generate weights for pseudo-new classes:

      
$$G \leftarrow \varphi_{\text{BiAG}}(\mathbf{p}_{old}^0, \mathbf{p}_{new}^0, W_{old}^0)$$

▷ Eq.(3)

12:  Compute analogical loss:

      
$$\mathcal{L}_G = 1 - \frac{G \cdot W_{new}^{0\top}}{\|G\| \cdot \|W_{new}^0\|}$$

▷ Eq.(4)

13:  Backpropagate and update BiAG parameters
14: end for
15: Freeze  $\varphi_{\text{BiAG}}(\cdot)$ 

16: Step 3: Weight Generation for New Classes (Sessions
     $t = 1$  to  $T$ )
17: for each session  $t = 1$  to  $T$  do
18:   Extract prototypes  $\mathbf{p}^t$  from  $\mathcal{D}^t$  using frozen  $f(\cdot)$ 
19:   Generate new class weights:

      
$$W^t \leftarrow \varphi_{\text{BiAG}}(\mathbf{p}^{0:t-1}, \mathbf{p}^t, W^{0:t-1})$$

▷ Eq.(5)

20:   Update classifier by concatenating weights:

      
$$W^{0:t} \leftarrow \text{Concat}(W^{0:t-1}, W^t)$$

▷ Eq.(6)

21:   Evaluate on  $\mathcal{Z}^{0:t}$ 
22: end for
23: return Final classification weights  $W^{0:T}$ 

```

Additionally, our approach of randomly selecting \mathcal{C}_{new}^0 for multiple rounds of repeated training helps mitigate the bias introduced by the randomness of class selection, thereby enhancing the robustness of analogical generation.

3) *Weight Generation for New Classes*: In this stage, both the feature extractor $f(\cdot)$ and the analogical generator BiAG $\varphi_{\text{BiAG}}(\cdot)$ are frozen to preserve the previously acquired knowledge. The goal is to generate classification weights for newly emerged classes using only a few labeled samples. This is achieved by analogically leveraging the semantic and structural knowledge encoded in the prototypes and weights of old classes.

When new classes appear in session t , we first extract the prototypes \mathbf{p}^t of the new classes using the frozen feature extractor $f(\cdot)$. These prototypes capture the central representation of each new class. At the same time, we maintain the

prototypes $\mathbf{p}^{0:t-1} = [\mathbf{p}^0, \dots, \mathbf{p}^{t-1}]$ and classification weights $W^{0:t-1} = \{W^i\}_{i=0}^{t-1}$ of all previously seen classes.

Then, we input the old class knowledge—i.e., $\mathbf{p}^{0:t-1}$ and $W^{0:t-1}$ —along with the new prototypes \mathbf{p}^t into BiAG to generate the classification weights W^t for the new classes:

$$W^t = \varphi_{\text{BiAG}}(\mathbf{p}^{0:t-1}, \mathbf{p}^t, W^{0:t-1}) \quad (5)$$

This process can be viewed as a form of cognitive analogy, where the system constructs an understanding of the new classes by relating them to known ones in the learned semantic space.

Compared to fine-tuning or storing exemplars, this strategy provides a flexible and efficient mechanism for incorporating novel categories. It avoids direct parameter updates and minimizes interference with previously learned knowledge, which is crucial for preventing catastrophic forgetting in FSCIL scenarios.

Finally, we update the classifier by concatenating the new weights with the previous weights:

$$W^{0:t} = \text{Concat}[W^{0:t-1}, W^t] \quad (6)$$

This updated weight matrix $W^{0:t}$ is then used for classification across all classes encountered from session 0 to t .

C. Brain-inspired Analogical Generator

Inspired by the prefrontal cortex’s capacity for abstract reasoning and relational mapping, as shown in Fig.3, BiAG integrates three specialized modules to emulate analogical reasoning: the Weight Self-Attention module (WSA), the Weight & Proto Analogical Attention (WPAA), and the Semantic Conversion module (SCM).

1) *Semantic conversion module (SCM)*: The SCM transforms the semantics of learnable queries between prototypes and weights based on Neural Collapse theory. According to Neural Collapse theory [57], during the terminal phase of deep neural network training, features of samples from the same class collapse to their class mean, and these class means (prototypes) become symmetrically arranged as a simplex ETF (Equiangular Tight Frame) centered at the origin. Simultaneously, the classification weight vectors align with their corresponding class prototypes, forming an almost identical geometric structure in the dual space—a phenomenon known as self-dual alignment. This alignment implies a tight coupling between the classification weights and the class prototypes, allowing them to be interchanged or mapped onto each other. This theoretical insight directly motivates the design of the Semantic Conversion Module (SCM) in the Brain-Inspired Analogical Generator (BiAG). By leveraging the correspondence between prototypes and classification weights revealed by Neural Collapse, SCM enables effective translation between feature space and classifier space. In essence, SCM is grounded in the understanding that class prototypes and classifier weights encode the same discriminative information, albeit in different forms.

The main function of SCM is to convert the semantics between prototypes and weights, thereby assisting the analogical learning process of BiAG. SCM employs a multi-layer

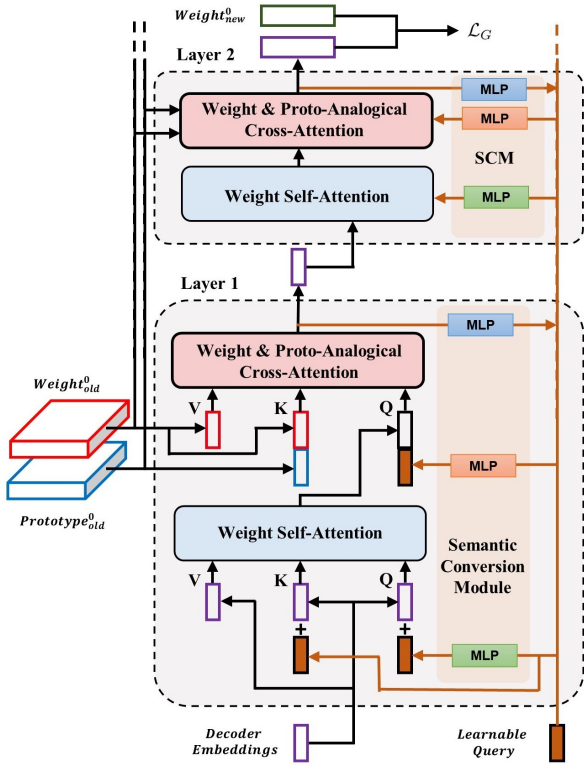


Fig. 3. The architecture of the proposed Brain-Inspired Analogical Generator (BiAG). BiAG consists of stacked layers of Weight Self-Attention and Weight & Proto-Analogical Cross-Attention modules. A shared Semantic Conversion Module (SCM) transforms learnable queries between prototype and weight semantics to facilitate analogical generation of new class weights.

perceptron (MLP) to transform the semantics of the learnable query from prototype to weight, or vice versa, to adapt to different learning stages. SCM inputs the learnable query with weight semantics after conversion into WSA for supplementary knowledge computation and inputs the learnable query with prototype semantics into WPAA for analogical learning. Additionally, SCM converts the output of the previous layer into class prototype semantics and adds it to the learnable query for updating.

2) *Weight Self Attention (WSA)*: The Weight Self-Attention (WSA) module is designed to enhance the weights of new classes by supplementing relevant knowledge. WSA selectively focuses on important features in the input data through a self-attention mechanism, thereby improving the representational capacity of the new class weights. Additionally, WSA introduces a learnable query $q_L \in \mathbb{R}^{c^t \times D}$ to further enhance the efficiency of utilizing new class knowledge. The learnable query is initialized with the prototype of the new class $p^t \in \mathbb{R}^{c^t \times D}$ and transformed into weights by the SCM to ensure the correct semantic representation and accurate expression of new class information:

$$q_W = \varphi_{\text{SCM}}(q_L) \quad (7)$$

Next, the WSA module takes the decoder embedding d_E and the obtained q_W as inputs to obtain the supplementary

knowledge W_s for the new class weights:

$$Q_s = q_W + d_E, K_s = q_W + d_E, V_s = d_E \quad (8)$$

$$W_s = \text{softmax}\left(\frac{Q_s \cdot K_s^T}{\sqrt{D}}\right) \cdot V_s. \quad (9)$$

where D is the dimension of the decoder embedding. WSA enhances the efficiency of knowledge utilization by performing self-attention processing on d_E and q_W , supplementing the knowledge related to new class weights. The supplementary knowledge generated by WSA aids in efficiently learning new classes with minimal data, providing a more comprehensive understanding of the new classes.

3) *Weight & Proto Analogical Attention (WPAA)*: The role of the WPAA, as shown in Fig.3, is to analogize between old knowledge and new knowledge, thereby reorganizing the old classification weights and generating the classification weights for new classes.

First, to enhance generative flexibility and assist in the analogy between new and old knowledge, the q_L is transformed into prototype semantics q_P through the SCM and then concatenated with the supplementary knowledge of new class weights W_s obtained from WSA:

$$q_P = \varphi_{\text{SCM}}(q_L), \quad (10)$$

$$z_t = \text{Concat}[W_s, q_P]. \quad (11)$$

Next, as shown in Fig.3, we use the obtained z_t as the query for WPAA. The classification weights of the already learned classes $W^{0:t-1} = \{W^i\}_{i=0}^{t-1} \in \mathbb{R}^{c^{0:t-1} \times D}$ are concatenated with their class prototypes $p^{0:t-1} \in \mathbb{R}^{c^{0:t-1} \times D}$ to serve as the key for WPAA. The classification weights of the already learned classes $W^{0:t-1}$ are used as the value:

$$Q_c = z_t = \text{Concat}[W_s, q_P], \quad (12)$$

$$K_c = \text{Concat}[W^{0:t-1}, p^{0:t-1}], \quad (13)$$

$$V_c = W^{0:t-1}, \quad (14)$$

$$W^t = \text{softmax}\left(\frac{Q_c \cdot K_c^T}{\sqrt{D}}\right) \cdot V_c. \quad (15)$$

where D is the dimension of the feature embedding. WPAA calculates the analogy between new and old classes using cross-attention, reorganizing old class weights to generate new class weights. The learnable query is crucial in this process, enhancing knowledge utilization efficiency and ensuring the accurate generation of new class weights.

For scalability, WPAA can be enhanced with SCM, which converts the previous layer's output into class prototype semantics and adds them to the learnable query for updates:

$$q_{L_n} = \varphi_{\text{SCM}}(W^t) + q_{L(n-1)} \quad (16)$$

Where n is the number of layers in BiAG. The WSA and WPAA parameters in each layer are independent, while SCM shares parameters across layers. This design ensures consistent semantic conversion and enhances the model's analogy capability through layer-by-layer optimization.

TABLE I

PERFORMANCE OF FSCIL IN EACH SESSION ON MINIIMAGENET AND COMPARISON WITH OTHER STUDIES. THE RESULTS WERE IMPLEMENTED BY [1], [5] IN THE FSCIL SETTING. “AVERAGE ACC.” IS THE AVERAGE ACCURACY OF ALL SESSIONS. “AVERAGE IMPROV.” INDICATES THE OVERALL IMPROVEMENT OF BIAG OVER EACH METHOD’S AVERAGE ACCURACY. “FINAL IMPROV.” CALCULATES THE IMPROVEMENT OF OUR METHOD IN THE LAST SESSION.

Method	Acc. in each session (%) \uparrow									Average	Average	Final
	0	1	2	3	4	5	6	7	8	ACC.	Improv.	Improv.
TOPIC (CVPR-2020)	61.31	50.09	45.17	41.16	37.48	35.52	32.19	29.46	24.42	39.64	+30.41	+35.41
SPPR (NeurIPS-2021)	61.45	63.80	59.53	55.53	52.50	49.60	46.69	43.79	41.92	52.76	+17.29	+17.91
ERL (AAAI-2021)	61.70	56.40	54.45	51.20	47.80	45.19	44.26	41.51	39.69	49.13	+20.92	+20.14
CEC (CVPR-2021)	72.00	66.83	62.97	59.43	56.70	53.73	51.19	49.24	47.63	57.75	+12.30	+12.20
ALICE (ECCV-2022)	80.60	70.60	67.40	64.50	62.50	60.00	57.80	56.80	55.70	63.99	+6.06	+4.13
CLOM (NeurIPS-2022)	73.08	68.09	64.16	60.41	57.41	54.29	51.54	49.37	48.00	58.48	+11.57	+11.57
MetaFSCI (CVPR-2022)	72.04	67.94	63.77	60.29	57.58	55.16	52.90	50.79	49.19	58.85	+11.20	+11.20
LIMIT (ECCV-2022)	72.32	68.47	64.30	60.78	57.95	55.07	52.70	50.72	49.19	59.06	+10.99	+10.99
FACT (CVPR-2022)	74.60	72.09	67.56	63.52	61.38	58.36	56.28	54.24	52.10	62.24	+7.81	+7.73
MCNet (CVPR-2023)	72.33	67.70	63.50	60.34	57.59	54.70	52.13	50.41	49.08	58.64	+11.41	+10.75
SubNet (CVPR-2023)	77.17	70.32	66.15	62.55	59.48	56.46	53.71	51.68	50.24	60.86	+9.19	+9.59
WaRP (CVPR-2023)	72.99	68.10	64.31	61.30	58.64	56.08	53.40	51.72	50.65	59.69	+10.36	+9.18
GKEAL (CVPR-2023)	73.59	68.90	65.33	62.29	59.39	56.70	54.20	52.29	51.31	60.45	+9.60	+8.52
BiDist (CVPR-2023)	76.65	70.42	66.29	62.77	60.75	57.24	54.79	53.65	52.22	61.64	+8.41	+7.61
SVAC (CVPR-2023)	81.12	76.14	72.43	68.92	66.48	62.95	59.92	58.39	57.11	67.05	+3.00	+2.72
ALFSCIL (TCSVT-2024)	81.27	75.97	70.97	66.53	63.46	59.95	56.93	54.81	53.31	64.92	+5.13	+6.52
NC-FSCIL (ICLR-2023)	84.02	76.80	72.00	67.83	66.35	64.04	61.46	59.54	58.31	67.82	+2.23	+1.52
KRRM (TCSVT-2024)	82.65	77.82	73.59	70.24	67.74	64.82	61.91	59.96	58.35	68.01	+2.04	+1.48
YourSelf (ECCV-2024)	84.00	<u>77.60</u>	<u>73.70</u>	<u>70.00</u>	<u>68.00</u>	<u>64.90</u>	<u>62.10</u>	<u>59.80</u>	<u>59.00</u>	<u>68.80</u>	+1.25	+0.83
BiAG (Ours)	84.78	80.14	75.43	71.48	68.76	65.81	62.99	61.20	59.83	70.05	–	–

IV. EXPERIMENTS

A. Datasets

Following standard FSCIL benchmarks, we evaluate our method on three widely used datasets: CIFAR-100, *miniImageNet*, and CUB-200, each with distinct characteristics and evaluation protocols.

CIFAR-100 consists of 100 general object categories with relatively low image resolution. In our setting, the base training set \mathcal{D}^0 contains 60 labeled classes, which are used for initial supervised training. The remaining 40 classes are divided into incremental sessions. In each session $t > 0$, 5 new classes are introduced with only 5 labeled samples per class, following a 5-way 5-shot format.

miniImageNet also includes 100 image categories and serves as a popular benchmark for few-shot learning. Similar to CIFAR-100, we adopt 60 classes as the base set \mathcal{D}^0 and use the remaining 40 classes for incremental learning. Each incremental session adds 5 new classes, with 5 labeled samples per class, maintaining the 5-way 5-shot configuration.

CUB-200 is a fine-grained dataset containing 200 bird species, characterized by high intra-class similarity and small inter-class variance, making it more challenging for FSCIL. For this dataset, the base training set \mathcal{D}^0 consists of 100 known classes. The remaining 100 classes are presented incrementally in 10 sessions, each introducing 10 novel classes with 5 labeled samples per class, following a 10-way 5-shot format.

This three-dataset evaluation protocol allows us to assess model performance under both generic and fine-grained FSCIL scenarios and to evaluate its ability to generalize across different levels of visual granularity with limited supervision.

B. Implementation Details

We adopt ResNet-12 and ResNet-18 [58] as feature extraction backbones in our experiments, following common practice in the FSCIL literature [49]. Specifically, ResNet-12 is employed for experiments on *miniImageNet* due to its widespread use in few-shot learning settings, while ResNet-18 is used for CIFAR-100 and CUB-200, consistent with prior FSCIL benchmarks.

During the base session training, we apply standard data preprocessing and augmentation techniques to improve generalization. These include random scaling, horizontal flipping, and CutMix [5], [59], which have been shown to be effective in reducing overfitting, especially in low-data regimes. The models are optimized using stochastic gradient descent (SGD) with a momentum of 0.9 and a weight decay of 5×10^{-4} , a widely used configuration in previous FSCIL studies.

For training in the base session, we run 200 epochs on both CIFAR-100 and *miniImageNet*, using an initial learning rate of 0.1 and a batch size of 128. For the CUB-200 dataset, which is more fine-grained and prone to overfitting, we set the initial learning rate to 0.02 and reduced the batch size to 64 to stabilize training. The learning rate is decayed by a factor of 0.1 at 100 and 150 epochs. All models are trained on a single NVIDIA 3090 GPU using PyTorch. This consistent and well-established training setup ensures a fair comparison with prior FSCIL methods while allowing us to focus on evaluating the impact of our proposed analogical learning framework.

C. Comparison with State-of-the-Art Methods

We benchmark our method against a wide range of state-of-the-art (SOTA) FSCIL methods across three standard

TABLE II
PERFORMANCE OF FSCIL IN EACH SESSION ON CUB200 AND COMPARISON WITH OTHER STUDIES.

Method	Accuracy in each session (%) \uparrow										Average	Average	Final	
	0	1	2	3	4	5	6	7	8	9	10	ACC.	Improv.	Improv.
TOPIC (CVPR-2020)	68.68	62.49	54.81	49.99	45.25	41.40	38.35	35.36	32.22	28.31	26.28	43.92	+26.79	+37.44
ERL (AAAI-2021)	73.52	71.09	66.13	63.25	59.89	59.49	58.64	57.72	56.15	54.75	52.28	61.17	+9.54	+11.44
IDLQV (NeurIPS-2020)	77.37	74.72	70.28	67.13	65.34	63.52	62.10	61.54	59.04	58.68	57.81	65.23	+5.48	+5.91
SPPR (NeurIPS-2021)	68.68	61.85	57.43	52.68	50.19	46.88	44.65	43.07	40.17	39.63	37.33	49.32	+21.39	+26.39
CEC (CVPR-2021)	75.85	71.94	68.50	63.50	62.43	58.27	57.73	55.81	54.83	53.52	52.28	61.33	+9.38	+11.44
MgSvF (NeurIPS-2021)	72.29	70.53	67.00	64.92	62.67	61.89	59.63	59.15	57.73	55.92	54.33	62.37	+8.34	+9.39
LIMIT (ECCV-2022)	76.32	74.18	72.68	69.19	68.79	65.64	63.57	62.69	61.47	60.44	58.45	66.67	+4.04	+5.27
MetaFSCIL (CVPR-2022)	75.90	72.41	68.78	64.78	62.96	59.99	58.30	56.85	54.78	53.82	52.64	61.93	+8.78	+11.08
ALICE (ECCV-2022)	77.40	72.70	70.60	67.20	65.90	63.40	62.90	61.90	60.50	60.60	60.10	65.75	+4.96	+3.62
FACT (CVPR-2022)	75.90	73.23	70.84	66.13	65.56	62.15	61.74	59.83	58.41	57.89	56.94	64.42	+6.29	+6.78
WaRP (ICLR-2023)	77.74	74.15	70.82	66.90	65.01	62.64	61.40	59.86	57.95	57.77	57.01	64.66	+6.05	+6.71
Subnet (ICLR-2023)	78.14	74.61	71.28	67.46	65.12	62.39	60.84	59.17	57.41	57.12	56.64	64.56	+6.15	+7.08
GKEAL (CVPR-2023)	78.88	75.62	72.32	68.62	67.23	64.26	62.98	61.89	60.20	59.21	58.67	66.34	+4.37	+5.05
BiDist (CVPR-2023)	79.12	75.37	72.80	69.05	67.53	65.12	64.00	63.51	61.87	61.47	60.93	67.34	+3.37	+2.79
ALFSCIL (TCSVT-2024)	79.79	76.53	73.12	69.02	67.62	64.76	63.45	62.32	60.83	60.21	59.30	66.99	+3.72	+4.42
NC-FSCIL (ICLR-2023)	80.45	75.98	72.30	70.28	68.17	65.16	64.43	63.25	60.66	60.01	59.44	67.28	+3.43	+4.28
KRRM (TCSVT-2024)	79.46	76.11	73.12	69.31	67.97	65.86	64.50	63.83	62.20	62.00	60.97	67.85	+2.86	+2.75
SVAC (CVPR-2023)	81.85	77.92	74.95	70.21	69.96	67.02	66.16	65.30	63.84	63.15	62.49	69.35	+1.36	+1.23
Yourself (ECCV-2024)	83.40	77.00	75.30	72.20	69.90	66.80	66.00	65.60	64.10	64.50	63.60	69.80	+0.91	+0.12
BiAG (Ours)	<u>82.97</u>	79.75	76.56	<u>71.88</u>	70.72	68.30	68.55	66.49	64.63	<u>64.25</u>	63.72	70.71	–	–

TABLE III
PERFORMANCE OF FSCIL IN EACH SESSION ON CIFAR-100 AND COMPARISON WITH OTHER STUDIES.

Method	Acc. in each session (%) \uparrow									Average	Average	Final
	0	1	2	3	4	5	6	7	8	ACC.	Improv.	Improv.
TOPIC (CVPR-2020)	64.10	55.88	47.07	45.16	40.11	36.38	33.96	31.55	29.37	42.62	+26.31	+28.55
ERL (AAAI-2021)	73.62	66.79	63.88	60.54	56.98	53.63	50.92	48.73	46.33	57.94	+10.99	+11.62
SPPR (NeurIPS-2021)	64.10	65.86	61.36	57.45	53.69	50.75	48.58	45.66	43.25	54.52	+14.41	+14.62
LIMIT (ECCV-2022)	74.30	70.44	66.12	61.24	58.77	53.91	51.36	49.20	45.33	58.63	+10.30	+12.62
C-FSCIL (CVPR-2022)	77.47	72.00	66.54	61.39	58.10	55.12	52.47	50.47	47.11	60.74	+8.19	+10.84
Data-free Replay (CVPR-2022)	74.40	70.60	66.54	61.39	58.91	51.36	50.14	47.76	44.10	58.18	+10.75	+13.85
MetaFSCIL (CVPR-2022)	74.50	70.10	66.87	62.77	59.48	56.52	54.32	52.56	49.97	60.79	+8.14	+8.98
CLOM (NeurIPS-2022)	74.20	69.83	66.17	62.39	59.26	56.48	54.36	52.16	50.25	60.56	+8.37	+7.70
CEC (CVPR-2021)	73.07	68.88	65.26	61.19	58.09	55.57	53.22	51.34	49.14	59.53	+9.40	+8.81
ALICE (ECCV-2022)	79.00	70.50	67.10	63.40	61.20	59.20	58.10	56.30	54.10	63.16	+5.77	+3.85
FACT (CVPR-2022)	74.60	72.09	67.56	63.52	61.38	58.36	56.28	54.24	52.10	62.24	+6.69	+5.85
WaRP (ICLR-2023)	80.31	76.86	71.87	67.58	64.39	61.34	59.15	57.10	54.74	65.92	+3.01	+3.21
Subnet (ICLR-2023)	80.33	76.23	72.19	67.83	64.64	61.39	59.32	57.37	54.94	66.03	+2.90	+3.01
GKEAL (CVPR-2023)	74.01	70.45	67.01	63.08	60.01	57.30	55.50	53.39	51.40	61.35	+7.58	+6.55
SVAC (CVPR-2023)	78.77	73.31	69.31	64.93	61.70	59.25	57.13	55.19	53.12	63.63	+5.30	+4.83
BiDist (CVPR-2023)	79.45	75.20	71.34	67.40	64.50	61.05	58.73	56.73	54.31	65.41	+3.52	+3.64
ALFSCIL (TCSVT-2024)	80.75	<u>77.88</u>	72.94	68.79	65.33	62.15	60.02	57.68	55.17	65.81	+3.12	+2.78
KRRM (TCSVT-2024)	81.25	77.23	73.30	69.41	<u>66.69</u>	<u>63.93</u>	<u>62.16</u>	<u>59.62</u>	<u>57.41</u>	66.00	+2.93	+0.54
YourSelf (ECCV-2024)	<u>82.90</u>	76.30	72.90	67.80	65.20	62.00	60.70	58.80	56.60	67.02	+1.91	+1.35
NC-FSCIL (ICLR-2023)	82.52	76.82	<u>73.34</u>	<u>69.68</u>	66.19	62.85	60.96	59.02	56.11	<u>67.50</u>	+1.43	+1.84
BiAG (Ours)	84.00	78.97	74.73	70.75	67.36	64.21	62.21	60.20	57.95	68.93	–	–

datasets: *miniImageNet*, CIFAR-100, and CUB-200. The detailed session-wise results are reported in Tables I, II and III, respectively. These experiments follow the FSCIL protocol introduced in [1], where each incremental session introduces a small number of novel classes with limited labeled samples.

On *miniImageNet*, as presented in Table I, our method achieves the highest final session accuracy of 59.83% and the best average accuracy of 70.05%. Compared to *Yourself* and *NC-FSCIL*, two of the strongest recent methods, BiAG

achieves improvements of **1.25%** and **2.01%** in final accuracy and **0.83%** and **2.23%** in average accuracy, respectively. These consistent gains demonstrate the effectiveness of our analogical reasoning framework in maintaining discriminative power across incremental sessions, especially in the later stages where performance often degrades.

On CUB-200, a fine-grained dataset with high intra-class similarity, our method achieves a final session accuracy of 63.72% and an average accuracy of 70.71%, as detailed in

TABLE IV
PERFORMANCE COMPARISON OF DIFFERENT METHODS.

Method	Average Base Acc.	Average Final ACC.	Average Avg Acc.
TOPIC (CVPR-2020)	64.70	26.69	42.06
ERL (AAAI-2021)	69.61	46.10	56.08
SPPR (NeurIPS-2021)	64.74	40.83	52.20
LIMIT (ECCV-2022)	74.31	50.99	61.45
CEC (CVPR-2021)	73.64	49.68	59.54
ALICE (ECCV-2022)	79.00	56.63	64.30
FACT (CVPR-2022)	75.03	53.71	62.97
WaRP (ICLR-2023)	77.01	54.13	63.42
GKEAL (CVPR-2023)	75.49	53.79	62.71
SVAC (CVPR-2023)	80.58	57.57	66.68
BiDist (CVPR-2023)	78.41	55.82	64.80
ALFSCIL (TCSVT-2024)	80.60	55.93	65.91
SVAC (CVPR-2023)	80.58	57.57	66.68
KRRM (TCSVT-2024)	81.12	58.91	67.29
NC-FSCIL (ICLR-2023)	82.33	57.95	67.53
Yourself (ECCV-2024)	<u>83.43</u>	<u>59.73</u>	<u>68.54</u>
BiAG (Ours)	83.92	60.50	69.90

Table II. Compared to SVAC, BiAG shows an improvement of **1.36%** in final accuracy and **1.23%** in average accuracy. Notably, BiAG also surpasses *Yourself*, indicating its capacity to handle fine-grained incremental learning with stronger semantic consistency. These results highlight that our method not only performs well on general datasets but also excels under more challenging fine-grained scenarios.

On CIFAR-100, as shown in Table III, BiAG obtains a final accuracy of 57.95% and an average accuracy of 68.93%, outperforming *Yourself* by **1.35%** in the final session and **1.91%** on average. The performance gain over *NC-FSCIL* is also clear, with improvements of **1.84%** in final accuracy and **1.43%** in average accuracy. This result reflects the robustness of our approach in more challenging settings with lower-resolution images and greater inter-class diversity, where many existing methods suffer from severe forgetting or limited generalization.

Across all three benchmarks, we report the average base session accuracy, final session accuracy, and overall average accuracy to comprehensively evaluate the performance of different methods under the FSCIL setting. As summarized in Table IV, our method BiAG consistently achieves the best results across all three metrics. In terms of **Average final session accuracy**, which reflects the model’s ability to retain base knowledge while integrating new classes over time, BiAG achieves **60.50%**. This clearly exceeds *Yourself* and KRRM, suggesting that our method suffers less from catastrophic forgetting and is more stable throughout incremental sessions. For the **overall average accuracy**, BiAG again achieves the highest score of **69.90%**, demonstrating superior performance across all sessions. This result surpasses both *Yourself* and *NC-FSCIL*, achieving relative improvements of **1.36%** and **2.37%**, respectively. These consistent improvements across all metrics highlight the robustness, generalization, and effectiveness of the proposed analogical reasoning framework. BiAG is not only capable of building strong initial representations but also

TABLE V
PERFORMANCE OF BASE AND NEW CLASSES ON THREE DATASETS.

Method	Final Session Accuracy	Final Session Base Acc.	Final Session New Avg Acc.
CEC	49.35	68.78	25.17
SVAC	57.57	75.12	33.79
NC-FSCIL	<u>57.95</u>	<u>75.49</u>	<u>34.44</u>
BiAG (Ours)	60.50	78.34	36.21

TABLE VI
COMPARISON OF FINAL SESSION BASE AND NEW CLASS ACCURACY ON CIFAR-100. “-” INDICATES RESULTS NOT REPORTED IN [41], [42].

Method	Final Session Accuracy	Final Session Base Acc.	Final Session New Avg Acc.
CEC	49.10	67.90	20.90
FACT	52.10	-	-
LIMIT	51.23	-	-
SVAC	53.12	73.07	23.20
NC-FSCIL	<u>56.11</u>	<u>73.98</u>	<u>29.30</u>
BiAG (Ours)	57.95	76.88	29.56

TABLE VII
COMPARISON OF FINAL SESSION BASE AND NEW CLASS ACCURACY ON miniImageNet. “-” INDICATES RESULTS NOT REPORTED IN [41], [42].

Method	Final Session Accuracy	Final Session Base Acc.	Final Session New Avg Acc.
CEC	47.67	67.97	27.37
FACT	50.49	-	-
LIMIT	49.19	-	-
SVAC	57.11	74.64	30.82
NC-FSCIL	58.31	76.30	31.33
BiAG (Ours)	59.83	79.58	30.21

excels in retaining knowledge and adapting to new categories in both general and fine-grained FSCIL scenarios.

D. Performance on Base and Novel Classes

We evaluate BiAG’s ability to learn novel classes while preserving old knowledge on three FSCIL benchmarks: *miniImageNet*, CIFAR-100, and CUB-200. To comprehensively assess performance, we report the following metrics in the final session: (1) **Final Session Accuracy**, which reflects the overall accuracy across all classes (base and novel) in the final session; (2) **Final Session Base Acc**, the accuracy restricted to base classes, indicating the model’s resistance to forgetting; (3) **Final Session New Avg Acc**, the average accuracy over all novel classes introduced during incremental learning; and (4) *Final Session New Acc*, the accuracy on the final 5-way novel classes, reported for CUB-200 to compare with methods like OrCo [51] that only provide this metric.

As shown in Table V, BiAG achieves the best results across all three datasets, demonstrating superior overall performance and balance. It reaches 60.50% final session accuracy, 78.34% base accuracy, and 36.21% new class average accuracy—outperforming NC-FSCIL by **2.55%** on base ac-

TABLE VIII
COMPARISON OF LAST SESSION BASE CLASSES ACCURACY, LAST SESSION NEW CLASSES ACCURACY, LAST SESSION NEW CLASSES AVERAGE ACCURACY, AND AVERAGE ACCURACY ON CUB-200. “-”: RESULTS NOT REPORTED IN ORCo [51]

Method	Final Session Acc.	Final Session Base Acc.	Final Session New Avg Acc.	Final Session New Acc.	Average Acc.
CEC (CVPR-2021)	52.12	70.46	33.78	34.23	61.33
FACT (CVPR-2022)	56.94	73.90	39.98	40.50	62.42
LIMIT (ECCV-2022)	57.41	73.60	41.22	41.80	66.67
ALFSCIL (TCSVT-2024)	59.30	74.21	44.39	45.17	66.99
NC-FSCIL (ICLR-2023)	59.44	73.98	44.90	45.83	67.28
OrCo (CVPR-2024)	-	66.62	-	49.25	62.36
SVAC (CVPR-2023)	62.50	77.65	47.35	47.68	69.61
BiAG (Ours)	63.72	78.57	48.87	49.36	70.71

curacy and **1.77%** on new average accuracy. These results highlight that BiAG provides a robust and scalable framework for FSCIL, exhibiting consistently strong performance in both knowledge retention and novel class generalization. Its effectiveness across diverse datasets and evaluation metrics validates the strength of our analogical learning strategy.

On **CIFAR-100** (Table VI), BiAG achieves the best performance across all three metrics—final session accuracy, base class accuracy, and novel class average accuracy. It outperforms NC-FSCIL in every aspect, demonstrating a superior balance between knowledge retention and adaptation and validating its robustness. On **miniImageNet** (Table VII), BiAG also achieves the highest overall and base class accuracy, surpassing NC-FSCIL by **3.28%** in base retention.

On the fine-grained benchmark **CUB-200** (Table VIII), BiAG achieves SOTA performance across all evaluation metrics. Compared with SVAC, one of the strongest prior methods, BiAG yields a clear improvement of **1.22%** in final session base class accuracy and **1.52%** in the average accuracy across all novel classes in the final session. In the final 5-way incremental step, BiAG achieves 49.36% accuracy, exceeding OrCo, which focuses more on improving performance for the currently added novel classes. These results underline BiAG’s effectiveness in fine-grained FSCIL settings, where classes often exhibit high visual similarity. The consistent improvements across both old and new classes suggest that BiAG not only retains previously learned knowledge but also excels at distinguishing subtle differences among closely related new categories.

E. Ablation Study

To better understand the design and effectiveness of the proposed Brain-Inspired Analogical Generator (BiAG), we conduct extensive ablation studies on three FSCIL benchmark datasets. We focus on evaluating the contributions of the core components, the effect of different network depths, and training configurations. The overall results are illustrated in Fig. 4 and detailed in Table IX.

1) *The Effectiveness of Each Component*: We evaluate the effectiveness of three key modules in BiAG: the Weight & Prototype Analogical Attention (WPAA), the Weight Self-Attention (WSA), and the Semantic Conversion Module

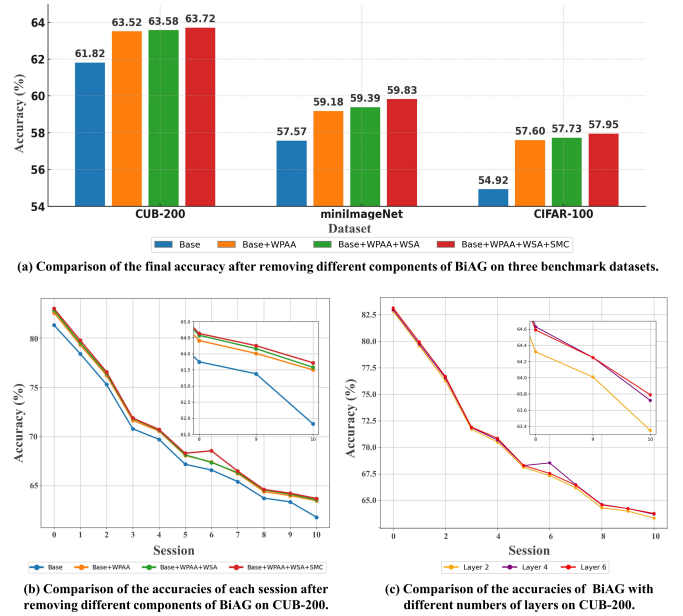


Fig. 4. The results of ablation experiments. Ablation studies on the proposed BiAG. (a) Final session accuracy on three datasets after incrementally adding key components (WPAA, WSA, SMC); (b) Session-wise accuracy comparison on CUB-200, showing the contribution of each component throughout the incremental process; (c) Accuracy comparison of BiAG with different numbers of layers, demonstrating that a deeper design improves generalization to new classes.

(SMC). As illustrated in Fig. 4(a), the addition of each component leads to a consistent and progressive improvement in final session accuracy across all three benchmarks, confirming their complementary roles.

Among the three, WPAA contributes the most significant performance gain. It provides a mechanism to establish analogical associations between new class prototypes and previously learned semantic structures, enabling effective weight generation even under limited supervision. As shown in Fig. 4(a), adding WPAA improves the final session accuracy by 1.70% on CUB-200, 1.61% on miniImageNet, and 2.68% on CIFAR-100 over the base model. However, when used in isolation, the improvements diminish in later sessions, suggesting limited temporal stability. Adding WSA on top of WPAA introduces

TABLE IX

ABLATION STUDY ON CIFAR-100 SHOWING THE INDIVIDUAL AND COMBINED EFFECTS OF THE WPAA, WSA, AND SMC MODULES WITHIN BiAG. WE REPORT THE ACCURACY FOR EACH SESSION, THE OVERALL AVERAGE ACCURACY (AVERAGE ACC), THE IMPROVEMENT OVER THE BASELINE (AVERAGE IMPROV), AND THE ACCURACY GAIN IN THE FINAL SESSION (FINAL IMPROV.).

WPAA	WSA	SMC	Acc. in each session (%) \uparrow										Average	Average	Final
			0	1	2	3	4	5	6	7	8	Acc.	Improv.	Improv.	
\times	\times	\times	84.00	65.32	63.24	61.84	59.59	58.24	56.80	55.97	54.92	62.21	—	—	
\checkmark	\times	\times	84.00	70.32	67.47	65.25	62.94	61.82	60.60	58.98	57.60	65.44	+3.23	+2.68	
\checkmark	\checkmark	\times	84.00	71.83	70.24	66.75	64.61	63.48	61.24	60.41	57.73	66.70	+4.49	+2.81	
\checkmark	\checkmark	\checkmark	84.00	78.97	74.73	70.75	67.36	64.21	62.21	60.20	57.95	68.93	+6.72	+3.03	

weight-level relational modeling, which helps the model maintain more consistent predictions as the incremental process progresses. The performance benefits accumulate further with the inclusion of SMC, which enhances the semantic compatibility between the feature space and the classifier space. When all three modules are incorporated, BiAG obtains the highest final session accuracy across all benchmarks, achieving cumulative improvements of 1.90% on CUB-200, 2.26% on miniImageNet, and 3.03% on CIFAR-100.

The session-wise analysis in Fig. 4(b) reveals that WPAA significantly improves early-stage performance but suffers from growing degradation without additional modules. WSA alleviates this issue by reinforcing intra-weight consistency across sessions. SMC further stabilizes the learning process by aligning high-level semantics between features and weights, especially under growing distributional shifts. This trend is also supported by the results on CIFAR-100 in Table IX. The average accuracy increases from 62.21% (base) to 65.44% with WPAA, 66.70% with WSA, and 68.93% with all modules enabled—corresponding to an overall improvement of 6.72%. In the final session, the accuracy grows from 54.92% to 57.95%, confirming the effectiveness of our full analogical generation pipeline.

These findings confirm that all three modules play essential and complementary roles. WPAA is fundamental for analogical generation, WSA stabilizes weight interaction over time, and SMC improves semantic transfer. Together, they lead to more robust and generalizable weight generation throughout the incremental learning process.

2) *The Influence of the Number of Layers*: We further investigate the effect of BiAG’s model depth by varying the number of stacked layers on the CUB-200 dataset. As shown in Fig. 4(c), increasing the number of layers leads to consistent improvements in final session accuracy. Specifically, the two-layer variant achieves 63.35%, while the four-layer and six-layer models reach 63.72% and 63.79%, respectively. These results suggest that deeper designs help BiAG capture richer analogical patterns and better align new class weights with prior knowledge. However, the performance gain from four to six layers is marginal, indicating diminishing returns as the depth increases. This trend suggests that a four-layer BiAG offers a favorable balance between model capacity and computational efficiency, capturing most of the essential cross-class relational structure without overcomplicating the architecture.

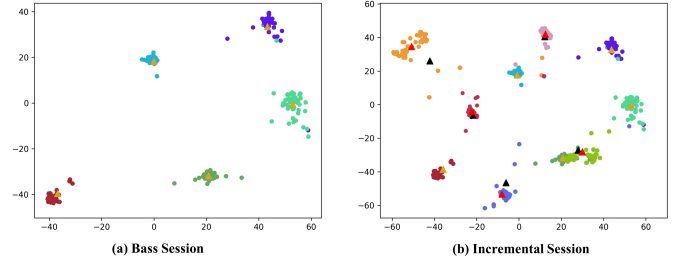


Fig. 5. t-SNE visualization on CIFAR-100. (a) Base session: clear class clusters aligned with classifier weights. (b) Incremental session: BiAG-generated weights (red) better match new class features than prototype-based weights (black), preserving structure and improving generalization.

F. Visualization

In Fig. 5, we visualize the feature distribution learned by our model using t-SNE [60] on the CIFAR-100 dataset. These visualizations offer an intuitive understanding of how BiAG organizes feature space across base and incremental sessions and how the generated weights help the model adapt to novel classes while retaining base knowledge.

Fig. 5(a) presents the feature representations after training on the base session. Each point corresponds to a sample, and different colors represent different base classes. The yellow triangles indicate the classifier weights learned for the base classes. As shown, samples of the same class are tightly clustered around their corresponding weights, forming clear and well-separated class boundaries. This indicates that the feature extractor successfully learns discriminative embeddings for base categories.

Fig. 5(b) shows the representations after an incremental session. In this case, black triangles denote the weights directly computed from new class prototypes, while red triangles denote the weights generated by BiAG. Notably, the generated weights (red) are more semantically aligned with the corresponding class clusters compared to the prototype-derived weights (black), which often deviate from the actual feature centers. This illustrates that BiAG can effectively leverage relational knowledge from old classes to generate more accurate and generalizable weights for novel classes.

Moreover, BiAG-generated weights not only improve the alignment of new class representations but also preserve the structure of the base class distribution. There is no significant shift or collapse in the base class clusters after incremental

learning, demonstrating the model’s resistance to catastrophic forgetting. This validates the effectiveness of our analogical generation mechanism in maintaining inter-class separation and ensuring stable learning across sessions. The visualization highlights how BiAG enables balanced and robust incremental learning by bridging semantic gaps between base and novel classes in the classifier space.

V. CONCLUSION AND FUTURE WORK

In this paper, we proposed the Brain-Inspired Analogical Generator (BiAG), a novel framework for Few-Shot Class-Incremental Learning (FSCIL). Drawing inspiration from human analogical reasoning, BiAG generates classification weights for novel classes by establishing semantic correspondences with previously learned knowledge—without requiring any parameter updates during incremental sessions. This design makes BiAG well-suited for data-scarce, dynamic learning scenarios. BiAG leverages old class weights, new prototypes, and a learnable query to produce semantically aligned weights via its three key components: WPAA, WSA, and SMC. These modules work together to improve generalization and reduce forgetting. Extensive experiments on CIFAR-100, miniImageNet, and CUB-200 show that BiAG consistently outperforms state-of-the-art methods across all key metrics, including average and final session accuracy.

In future work, we aim to explore the extension of this analogical generation paradigm to more complex continual learning scenarios. One direction is domain-incremental learning, where data from different distributions arrive sequentially, posing domain-shift challenges. Incorporating domain-aware analogical reasoning may enhance the model’s adaptability and robustness across heterogeneous environments. Additionally, integrating BiAG with more advanced backbone architectures or vision-language pretraining models (e.g., CLIP) may further enhance its semantic alignment capabilities, enabling few-shot incremental learning in open-vocabulary or multimodal settings. In summary, BiAG provides a new perspective on few-shot incremental learning through analogical reasoning. We believe this brain-inspired direction can inspire broader advancements in building flexible and cognitively motivated continual learning systems.

REFERENCES

- [1] X. Tao, X. Hong, X. Chang, S. Dong, X. Wei, and Y. Gong, “Few-shot class-incremental learning,” in *IEEE/CVF Conference on Computer Vision and Pattern Recognition*. IEEE, 2020, pp. 12 183–12 192.
- [2] Y. Zou, H. Zhang, L. Li, and Q. Li, “Boundary-based large margin classification for few-shot class-incremental learning,” in *Advances in Neural Information Processing Systems (NeurIPS)*, 2022.
- [3] Z. Chi, L. Gu, H. Liu, Y. Wang, Y. Yu, and J. Tang, “Metafscil: A meta-learning approach for few-shot class incremental learning,” in *IEEE/CVF Conference on Computer Vision and Pattern Recognition*. IEEE, 2022, pp. 14 166–14 175.
- [4] L. Chen *et al.*, “Bidist: Bi-level distillation for few-shot class-incremental learning,” *IEEE Transactions on Pattern Analysis and Machine Intelligence (PAMI)*, 2023.
- [5] C. Zhang, N. Song, G. Lin, Y. Zheng, P. Pan, and Y. Xu, “Few-shot incremental learning with continually evolved classifiers,” in *IEEE/CVF Conference on Computer Vision and Pattern Recognition*. IEEE, 2021, pp. 12 455–12 464.
- [6] A. Cheraghian, S. Rahman, G. Ramasinghe *et al.*, “Semantic-aware knowledge distillation for few-shot class-incremental learning,” in *Proceedings of the IEEE/CVF International Conference on Computer Vision (ICCV)*, 2021.
- [7] Z. Zhou, X. Wang *et al.*, “Forward compatible training for few-shot class-incremental learning,” in *Proceedings of the IEEE/CVF Conference on Computer Vision and Pattern Recognition (CVPR)*, 2022.
- [8] Z. Song, Y. Zhao, Y. Shi, P. Peng, L. Yuan, and Y. Tian, “Learning with fantasy: Semantic-aware virtual contrastive constraint for few-shot class-incremental learning,” in *IEEE/CVF Conference on Computer Vision and Pattern Recognition*. IEEE, 2023, pp. 24 183–24 192.
- [9] D. Hofstadter *et al.*, “Analogy as the core of cognition,” *The Analogical Mind*, 2001.
- [10] D. Gentner, “Analogy and abstraction,” *Topics in Cognitive Science*, 2017.
- [11] H. C. Barron, R. J. Dolan, and T. E. Behrens, “Online evaluation of novel choices by simultaneous representation of multiple memories,” *Nature neuroscience*, vol. 16, no. 10, pp. 1492–1498, 2013.
- [12] S. A. Bunge and C. Wendelken, “Analogical reasoning and prefrontal cortex: evidence for separable retrieval and integration mechanisms,” *Cerebral Cortex*, vol. 19, no. 5, pp. 922–933, 2009.
- [13] R. Lamprecht and J. E. LeDoux, “Structural plasticity and memory,” *Nature Reviews Neuroscience*, vol. 5, no. 1, pp. 45–54, 2004.
- [14] Z. Li and D. Hoiem, “Learning without forgetting,” *IEEE Transactions on Pattern Analysis and Machine Intelligence*, vol. 40, no. 12, pp. 2935–2947, 2017.
- [15] F. Zenke, B. Poole, and S. Ganguli, “Continual learning through synaptic intelligence,” *Proceedings of the 34th International Conference on Machine Learning*, pp. 3987–3995, 2017.
- [16] J. Kirkpatrick, R. Pascanu, N. Rabinowitz *et al.*, “Overcoming catastrophic forgetting in neural networks,” *Proceedings of the National Academy of Sciences*, vol. 114, no. 13, pp. 3521–3526, 2017.
- [17] H. Wen, H. Qiu, L. Wang, H. Cheng, and H. Li, “Class incremental learning with less forgetting direction and equilibrium point,” *IEEE Transactions on Circuits and Systems for Video Technology*, 2025.
- [18] S.-A. Rebuffi, A. Kolesnikov, G. Sperl, and C. H. Lampert, “icarl: Incremental classifier and representation learning,” *IEEE Conference on Computer Vision and Pattern Recognition (CVPR)*, pp. 5533–5542, 2017.
- [19] D. Lopez-Paz and M. Ranzato, “Gradient episodic memory for continual learning,” *Advances in Neural Information Processing Systems (NeurIPS)*, pp. 6467–6476, 2017.
- [20] D. Rolnick, A. Ahuja, J. Schwarz, T. Lillicrap, and G. Wayne, “Experience replay for continual learning,” *Advances in neural information processing systems*, vol. 32, 2019.
- [21] A. Chaudhry, M. Rohrbach, M. Elhoseiny, T. Ajanthan, P. K. Dokania, P. H. Torr, and M. Ranzato, “On tiny episodic memories in continual learning,” *arXiv preprint arXiv:1902.10486*, 2019.
- [22] H. Shin, J. K. Lee, J. Kim, and J. Kim, “Continual learning with deep generative replay,” in *Advances in Neural Information Processing Systems*, vol. 30, 2017.
- [23] K. Song, G. Liang, Z. Chen, and Y. Zhang, “Non-exemplar class-incremental learning by random auxiliary classes augmentation and mixed features,” *IEEE Transactions on Circuits and Systems for Video Technology*, 2024.
- [24] Y. Xian, H. Yu, H. Li, and G. Wang, “Class incremental learning via semantic information mapping and background information calibrating,” *IEEE Transactions on Circuits and Systems for Video Technology*, 2024.
- [25] D. Cheng, Y. Zhao, N. Wang, G. Li, D. Zhang, and X. Gao, “Efficient statistical sampling adaptation for exemplar-free class incremental learning,” *IEEE Transactions on Circuits and Systems for Video Technology*, 2024.
- [26] A. A. Rusu, N. C. Rabinowitz, G. Desjardins *et al.*, “Progressive neural networks,” *arXiv preprint arXiv:1606.04671*, 2016.
- [27] A. Mallya and S. Lazebnik, “Packnet: Adding multiple tasks to a single network by iterative pruning,” *IEEE Conference on Computer Vision and Pattern Recognition (CVPR)*, pp. 7765–7773, 2018.
- [28] J. Serra, D. Suris, M. Miron, and A. Karatzoglou, “Overcoming catastrophic forgetting with hard attention to the task,” in *International Conference on Machine Learning*. PMLR, 2018, pp. 4548–4557.
- [29] X. Gao, S. Dong, Y. He, Q. Wang, and Y. Gong, “Beyond prompt learning: Continual adapter for efficient rehearsal-free continual learning,” in *European Conference on Computer Vision*. Springer, 2024, pp. 89–106.
- [30] J. Yoon, E. Yang, J. Lee, and S. J. Hwang, “Lifelong learning with dynamically expandable networks,” *International Conference on Learning Representations (ICLR)*, 2018.

- [31] T. Xu and H. Zhu, “Reinforced continual learning,” *Advances in Neural Information Processing Systems (NeurIPS)*, pp. 899–908, 2018.
- [32] S. Dong, X. Gao, Y. He, Z. Zhou, A. C. Kot, and Y. Gong, “Ceat: Continual expansion and absorption transformer for non-exemplar class-incremental learning,” *IEEE Transactions on Circuits and Systems for Video Technology*, 2024.
- [33] R. Aljundi, F. Babiloni, M. Elhoseiny, M. Rohrbach, and T. Tuytelaars, “Expert gate: Lifelong learning with a network of experts,” in *Proceedings of the IEEE Conference on Computer Vision and Pattern Recognition*, 2017, pp. 3366–3375.
- [34] Z. Tao, L. Yu, H. Yao, S. Huang, and C. Xu, “Class incremental learning for light-weighted networks,” *IEEE Transactions on Circuits and Systems for Video Technology*, 2024.
- [35] B. Ni, X. Nie, C. Zhang, S. Xu, X. Zhang, G. Meng, and S. Xiang, “Mo-bo: Memory-boosted vision transformer for class-incremental learning,” *IEEE Transactions on Circuits and Systems for Video Technology*, 2024.
- [36] Y. Luo, H. Ge, Y. Liu, and C. Wu, “Representation robustness and feature expansion for exemplar-free class-incremental learning,” *IEEE Transactions on Circuits and Systems for Video Technology*, 2024.
- [37] S. Wang, W. Shi, S. Dong, X. Gao, X. Song, and Y. Gong, “Semantic knowledge guided class-incremental learning,” *IEEE Transactions on Circuits and Systems for Video Technology*, vol. 33, no. 10, pp. 5921–5931, 2023.
- [38] Z. Zhu, Z. Cao, D. Zhai, Y. Cheng, and Z. Zha, “Self-promoted prototype refinement for few-shot class-incremental learning,” in *Proceedings of the IEEE/CVF Conference on Computer Vision and Pattern Recognition (CVPR)*, 2021.
- [39] Z. Zhu, T. Ding, J. Zhou, X. Li, C. You, J. Sulam, and Q. Qu, “A geometric analysis of neural collapse with unconstrained features,” *Advances in neural information processing systems*, vol. 34, pp. 29 820–29 834, 2021.
- [40] K. Chen and C.-G. Lee, “Incremental few-shot learning via vector quantization in deep embedded space,” in *International Conference on Learning Representations*, 2020.
- [41] D.-W. Zhou, F.-Y. Wang, H.-J. Ye, L. Ma, S. Pu, and D.-C. Zhan, “Forward compatible few-shot class-incremental learning,” in *IEEE/CVF Conference on Computer Vision and Pattern Recognition*. IEEE, 2022, pp. 9046–9056.
- [42] D.-W. Zhou, H.-J. Ye, L. Ma, D. Xie, S. Pu, and D.-C. Zhan, “Few-shot class-incremental learning by sampling multi-phase tasks,” *IEEE Transactions on Pattern Analysis and Machine Intelligence*, 2022.
- [43] Y. Zou, S. Zhang, Y. Li, and R. Li, “Margin-based few-shot class-incremental learning with class-level overfitting mitigation,” *Advances in neural information processing systems*, vol. 35, pp. 27 267–27 279, 2022.
- [44] H. Zhuang, Z. Weng, R. He, Z. Lin, and Z. Zeng, “Gkeal: Gaussian kernel embedded analytic learning for few-shot class incremental task,” in *IEEE/CVF Conference on Computer Vision and Pattern Recognition*. IEEE, 2023, pp. 7746–7755.
- [45] L. Zhao, J. Lu, Y. Xu, Z. Cheng, D. Guo, Y. Niu, and X. Fang, “Few-shot class-incremental learning via class-aware bilateral distillation,” in *IEEE/CVF Conference on Computer Vision and Pattern Recognition*. IEEE, 2023, pp. 11 838–11 847.
- [46] H. Kang, J. Yoon, S. R. H. Madjid, S. J. Hwang, and C. D. Yoo, “On the soft-subnetwork for few-shot class incremental learning,” in *International Conference on Learning Representations*, 2023.
- [47] D.-Y. Kim, D.-J. Han, J. Seo, and J. Moon, “Warping the space: Weight space rotation for class-incremental few-shot learning,” in *International Conference on Learning Representations*, 2023.
- [48] Y. Wang, G. Zhao, and X. Qian, “Improved continually evolved classifiers for few-shot class-incremental learning,” *IEEE Transactions on Circuits and Systems for Video Technology*, vol. 34, no. 2, pp. 1123–1134, 2023.
- [49] Y. Yang, H. Yuan, X. Li, Z. Lin, P. Torr, and D. Tao, “Neural collapse inspired feature-classifier alignment for few-shot class-incremental learning,” in *International Conference on Learning Representations*, 2023.
- [50] H. Liu, L. Gu, Z. Chi, Y. Wang, Y. Yu, J. Chen, and J. Tang, “Few-shot class-incremental learning via entropy-regularized data-free replay,” in *European Conference on Computer Vision*. Tel Aviv, Israel: Springer, October 2022, pp. 146–162.
- [51] N. Ahmed, A. Kukleva, and B. Schiele, “Orco: Towards better generalization via orthogonality and contrast for few-shot class-incremental learning,” in *Proceedings of the IEEE/CVF Conference on Computer Vision and Pattern Recognition*, 2024, pp. 28 762–28 771.
- [52] Y.-M. Tang, Y.-X. Peng, J. Meng, and W.-S. Zheng, “Rethinking few-shot class-incremental learning: Learning from yourself,” in *European Conference on Computer Vision*. Springer, 2024, pp. 108–128.
- [53] J. Li, S. Dong, Y. Gong, Y. He, and X. Wei, “Analogical learning-based few-shot class-incremental learning,” *IEEE Transactions on Circuits and Systems for Video Technology*, 2024.
- [54] D. Gentner and J. Colhoun, “Analogical processes in human thinking and learning,” *Towards a theory of thinking: Building blocks for a conceptual framework*, pp. 35–48, 2010.
- [55] D. Gentner, “Structure-mapping: A theoretical framework for analogy,” in *Cognitive Science*, vol. 7, no. 2, 1983, pp. 155–170.
- [56] S. A. Bunge, J. D. Wallis, B. T. Parker *et al.*, “Analogical reasoning and prefrontal cortex: Evidence for relational integration and maintenance of semantic associations,” *Cerebral Cortex*, vol. 15, no. 5, pp. 489–497, 2004.
- [57] V. Pappayan, X. Han, and D. L. Donoho, “Prevalence of neural collapse during the terminal phase of deep learning training,” *Proceedings of the National Academy of Sciences*, vol. 117, no. 40, pp. 24 652–24 663, 2020.
- [58] K. He, X. Zhang, S. Ren, and J. Sun, “Deep residual learning for image recognition,” in *IEEE/CVF Conference on Computer Vision and Pattern Recognition*. IEEE, 2016, pp. 770–778.
- [59] S. Yun, D. Han, S. J. Oh, S. Chun, J. Choe, and Y. Yoo, “Cutmix: Regularization strategy to train strong classifiers with localizable features,” in *Proceedings of the IEEE/CVF international conference on computer vision*, 2019, pp. 6023–6032.
- [60] L. Van der Maaten and G. Hinton, “Visualizing data using t-sne,” *Journal of machine learning research*, vol. 9, no. 11, 2008.